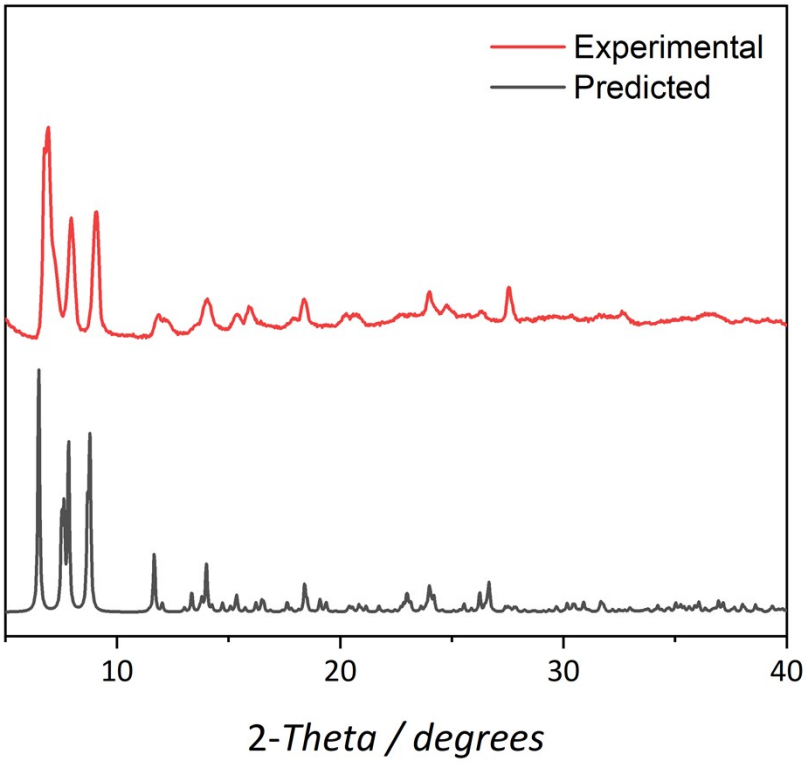

Figure S1. Experimental powder XRD data for compound **1** (red) and the simulated spectrum from the single crystal data (red).

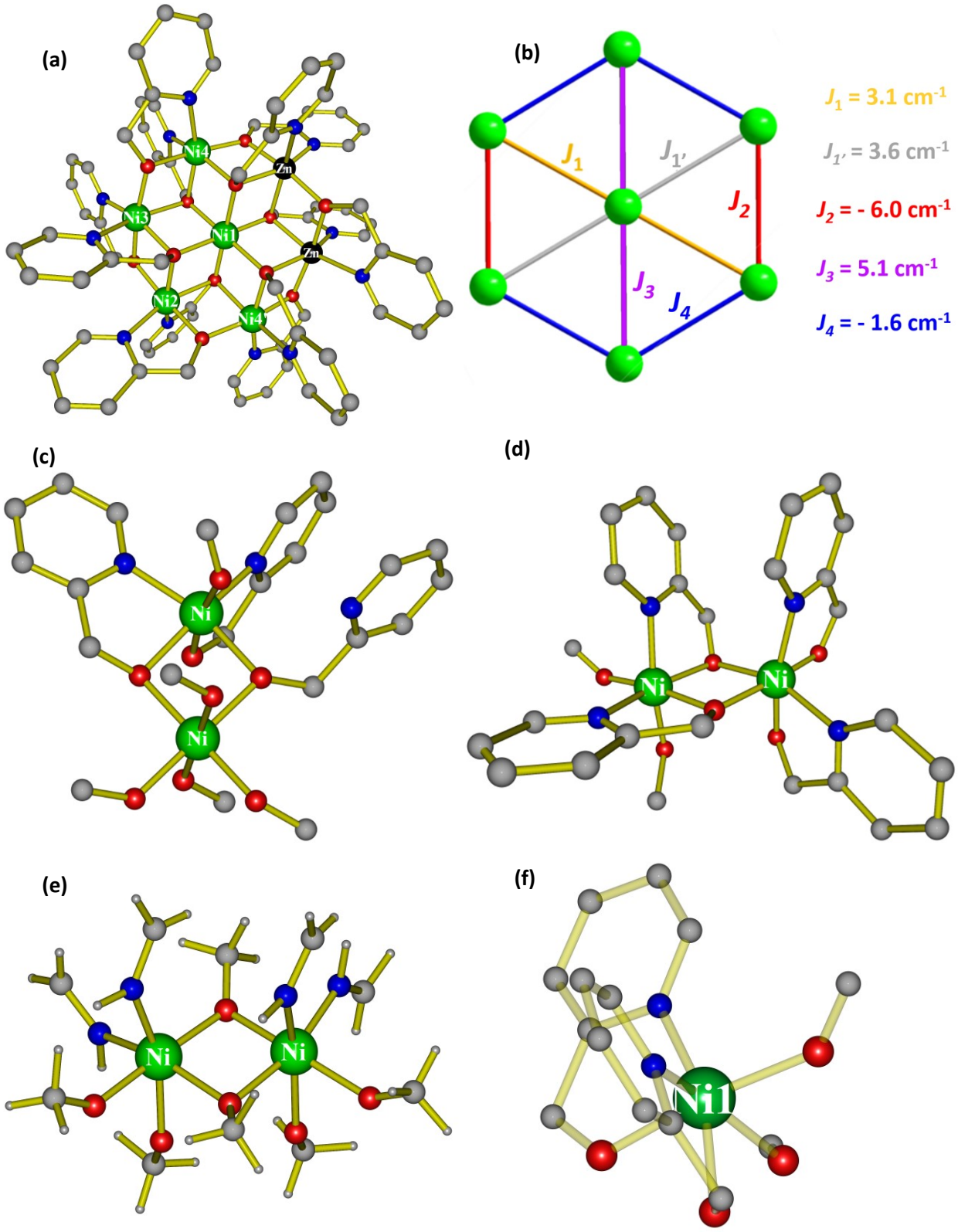
(a)
Ni4
Zn
Ni3
Ni1
Zn
Ni2
Ni4
(b)
J_1
$J_{1'}$
J_2
J_3
J_4
J_1 = 3.1 cm^{-1}
$J_{1'}$ = 3.6 cm^{-1}
J_2 = - 6.0 cm^{-1}
J_3 = 5.1 cm^{-1}
J_4 = - 1.6 cm^{-1}
(c)
Ni
Ni
(d)
Ni
Ni
(e)
Ni
Ni
(f)
Ni1

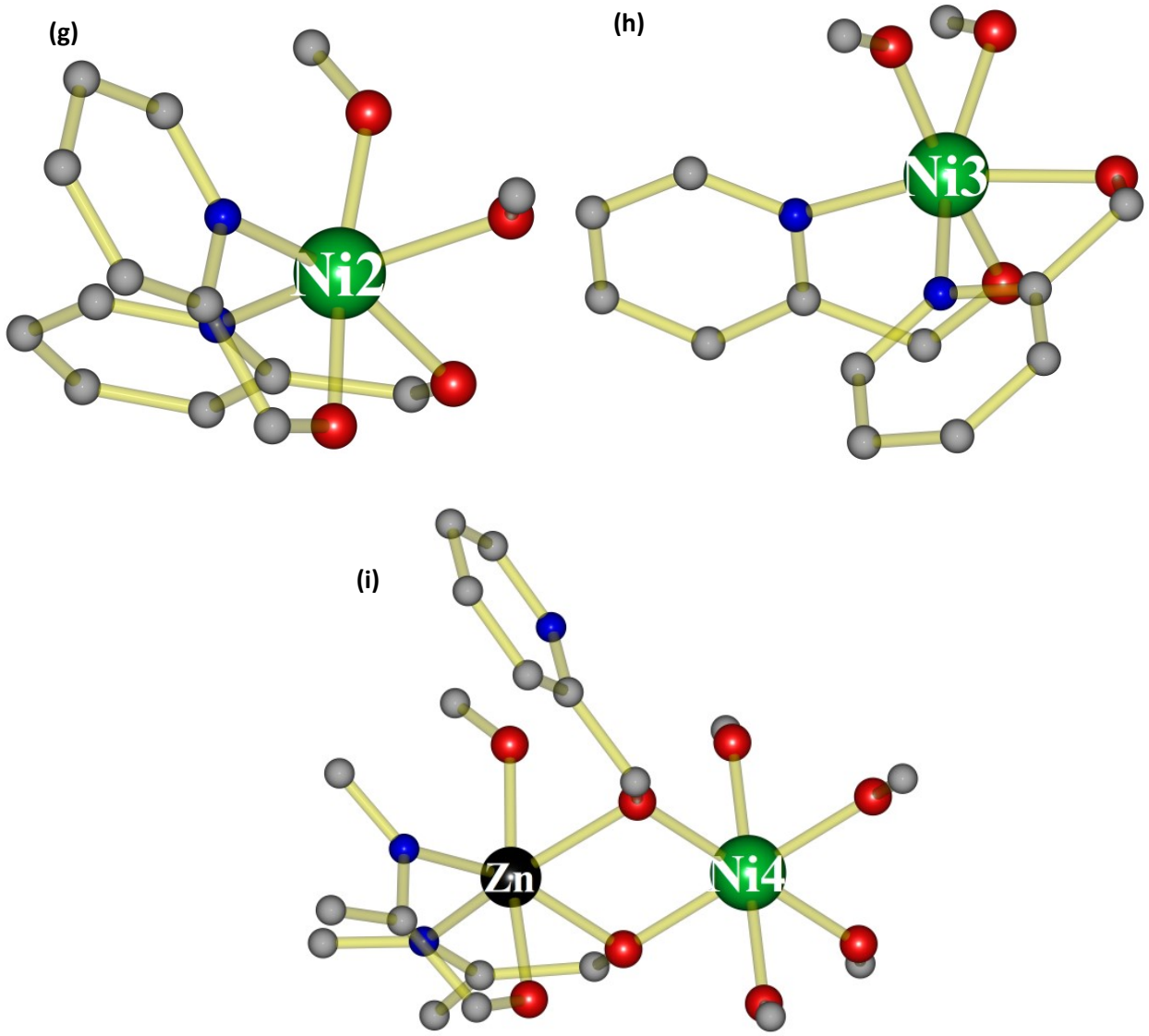

Figure S2. (a) The **[**Ni_5Zn_2] model created from the XRD structures of complex **1** employed to estimate the magnetic exchange interactions. (b) Magnetic exchange interaction model employed in the DFT calculations. (c-d) The dimetallic models **1A** and **1B** used respectively to estimate the magnetic exchange interactions between the central Ni(II) ion and the ring Ni(II) ions ($J_{\mathbf{1A}}$ = 8.2 cm^{-1}), and between the ring Ni(II) ions ($J_{\mathbf{1B}}$ =- 3.1 cm^{-1}), respectively. (e) The dimetallic models **1C** used to develop the magneto-structural correlation. (f-i) Chemical models **1D**-**1G** used to perform *ab initio* CASSCF/NEVPT2 calculations on the ring Ni(II) and central Ni(II) ions, respectively.

Table S1. Selected spin configurations used for estimating the magnetic exchange interactions in complex **1**. Note that the errors in the calculated *J* values are less than 0.3%. $\mathbf{E_{(HS\text{-}BS\text{-}i)}}$ values provide the relative energy (cm^{-1}) for spin configurations with respect to the spin configuration in which all Ni(II) ions align parallel (the high spin (HS) configuration).

Spin Configuration	Ni1	Ni2	Ni3	Ni4	Ni5	S (Total)	$E_{(HS\text{-}BS\text{-}i)}$ (cm^{-1}), i = 1-12
HS	**1**	**1**	**1**	**1**	**1**	**5**	
BS-1	**-1**	**1**	**1**	**1**	**1**	**3**	-23.2
BS-2	**1**	**-1**	**1**	**1**	**1**	**3**	-110.1
BS-3	**1**	**1**	**-1**	**1**	**1**	**3**	-20.1
BS-4	**1**	**1**	**1**	**-1**	**1**	**3**	-25.6
BS-5	**1**	**1**	**1**	**1**	**-1**	**3**	-28.4
BS-6	**-1**	**1**	**-1**	**1**	**1**	**1**	-49.5
BS-7	**-1**	**1**	**1**	**1**	**-1**	**1**	-49.6
BS-8	**1**	**-1**	**-1**	**1**	**1**	**1**	-81.2
BS-9	**1**	**-1**	**1**	**1**	**-1**	**1**	-77.6
BS-10	**1**	**1**	**-1**	**-1**	**1**	**1**	-48.9
BS-11	**1**	**1**	**-1**	**1**	**-1**	**1**	-47.8
BS-12	**1**	**1**	**1**	**-1**	**-1**	**1**	-60.6

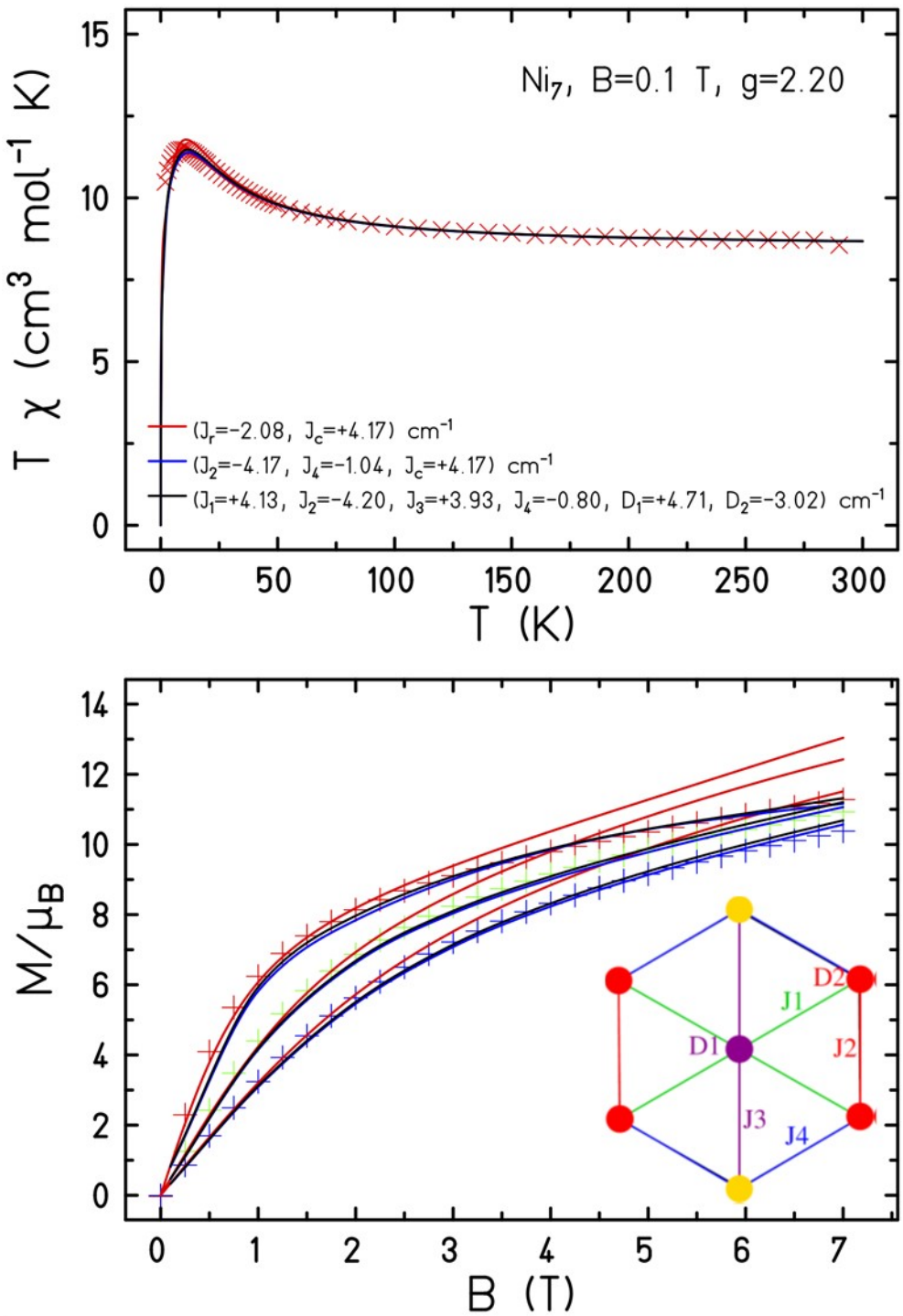

Figure S3. Plot of the χT product versus T (top) and M vs B (middle) for **1**. Exchange interaction model used to fit the magnetic susceptibility and magnetisation data for 1. J_1, J_3 represent J_{cr} interactions, J_2, J_4 represent J_{rr} interactions, and D_1 and D_2 represent the anisotropy of the central Ni ion and ring Ni ions, respectively (bottom).

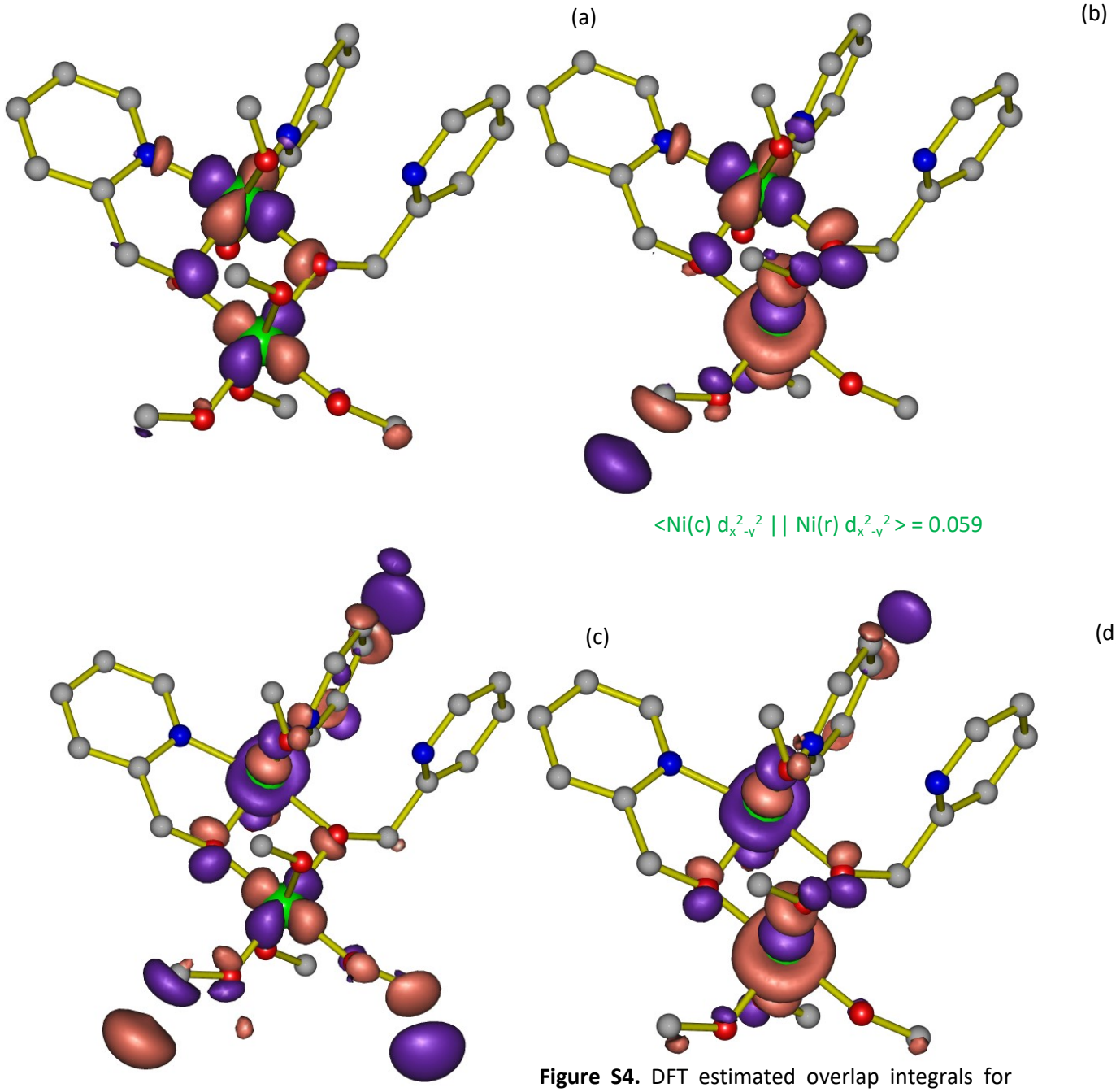

Figure S4. DFT estimated overlap integrals for model **1A**. One moderate (green text) and three weak (black text) overlap integrals result in a moderate ferromagnetic interaction between the central (Ni(c)) and ring (Ni(r)) metal centres ($J_{\mathbf{1A}}$ = 8.2 cm^{-1}).

<Ni(i) $d_{x^2-y^2}$ || Ni(r) d_{z^2} > = 0.032

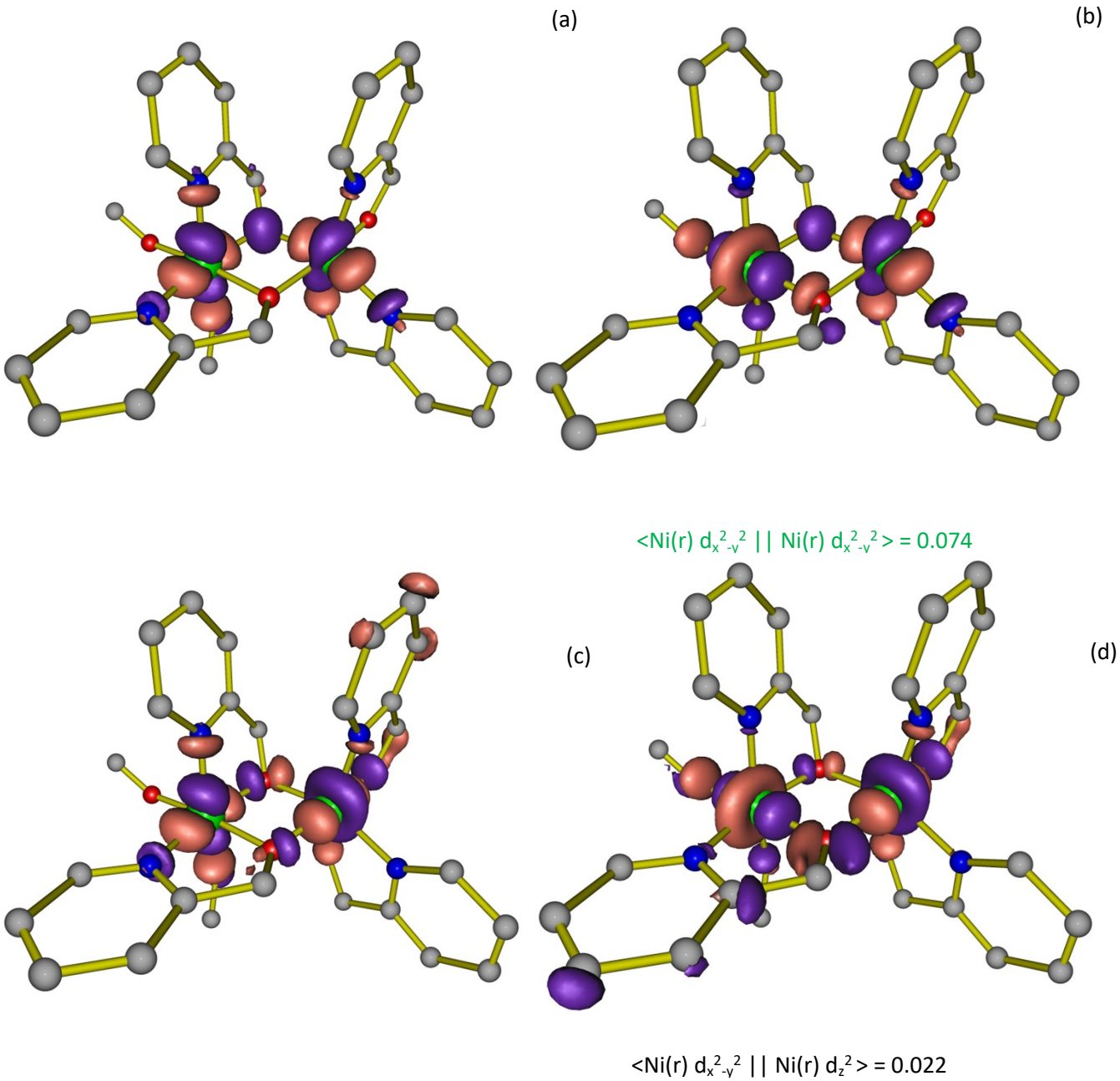

Figure S5. DFT estimated overlap integrals for model **1B**. Two moderate (green text) and two weak (black text) overlap integrals result in a weak antiferromagnetic interaction between central (Ni(c)) and ring (Ni(r)) metal centres ($J_{\mathbf{1B}}$ = -3.1 cm^{-1}).

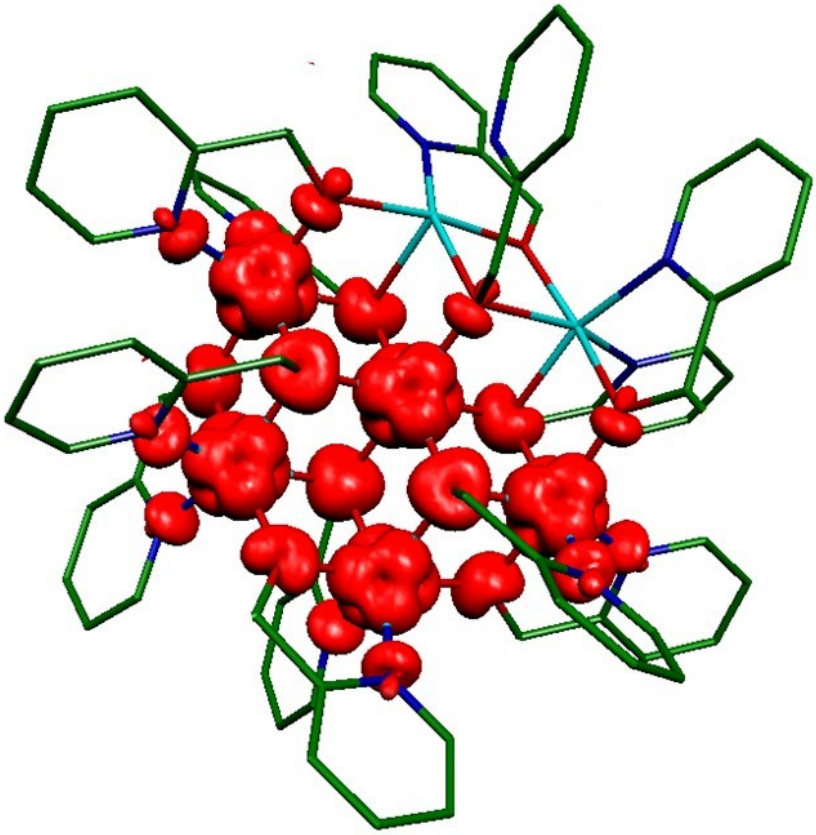

Figure S6. DFT estimated spin density plots for the Ni_5Zn_2 model (see Figure S1). Spin density analysis suggests strong delocalisation of spins onto the coordinating ligand atoms followed by weak spin polarisation. The iso-density surface is plotted with an 0.005 $e^-/bohr^3$ iso-value.

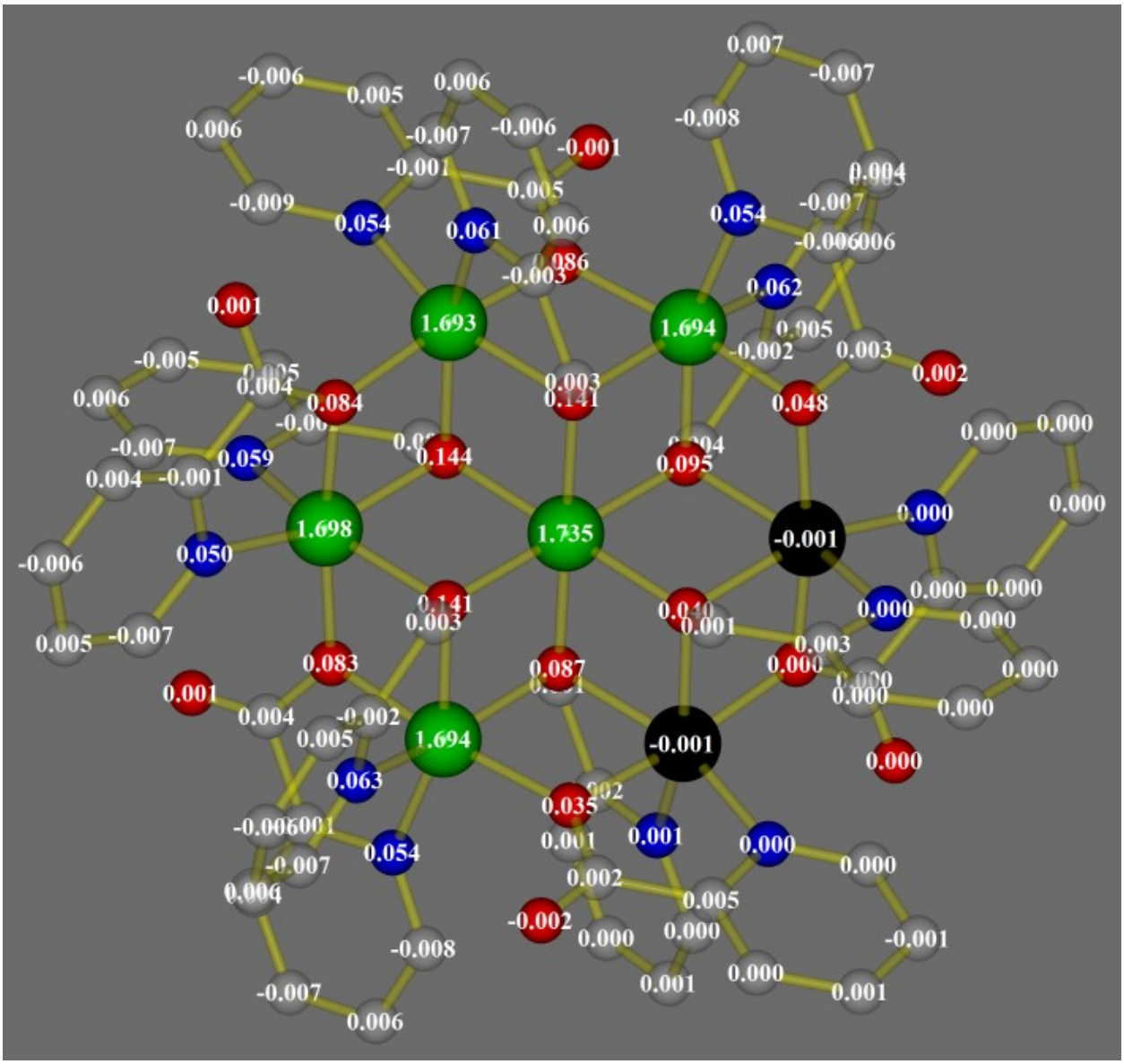

Figure S7. DFT estimated spin density values for the Ni_5Zn_2 model (see Figure S1). Spin density analysis suggest strong delocalisation of spins onto the coordinating ligand atoms followed by weak spin polarisation.

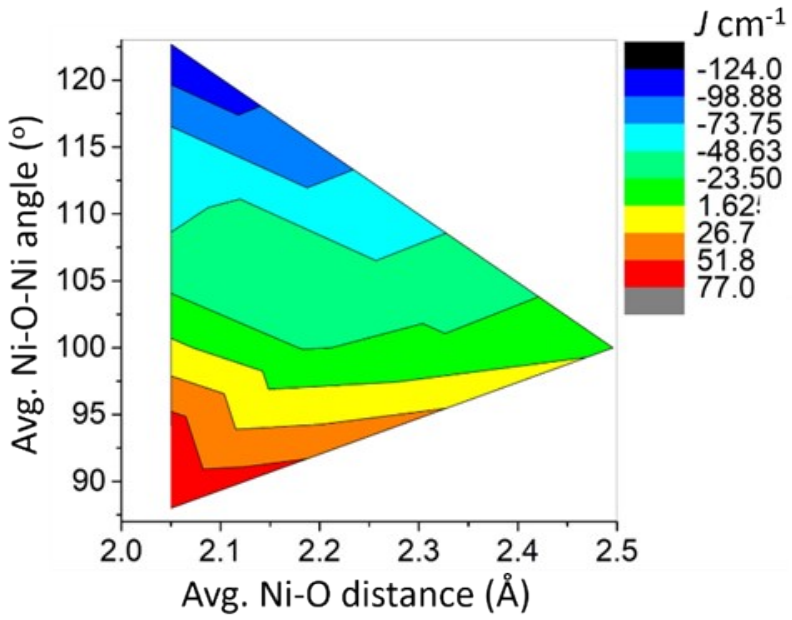

Figure S8. Magneto-structural correlation developed for model **1C** with respect to the average Ni-O-Ni angle and average Ni-O distance.

Table S2. Shape analysis performed on the Ni(II) ions of complex **1**.

HP-6	1 D_{6h}	Hexagon
PPY-6	2 C_{5v}	Pentagonal pyramid
OC-6	3 O_h	Octahedron
TPR-6	4 D_{3h}	Trigonal prism
JPPY-6	5 C_{5v}	Johnson pentagonal pyramid J2

Structure [ML_6]	HP-6	PPY-6	OC-6	TPR-6	JPPY-6
Ni1/Ni5 ,	32.969,	23.018,	1.806,	11.192,	27.212
Ni2/Ni6 ,	33.875,	22.080,	2.034,	10.271,	26.313
Ni3/Ni7 ,	33.273,	22.541,	1.744,	10.331,	26.655
Ni4 ,	24.861,	26.623,	0.878,	16.389,	29.489

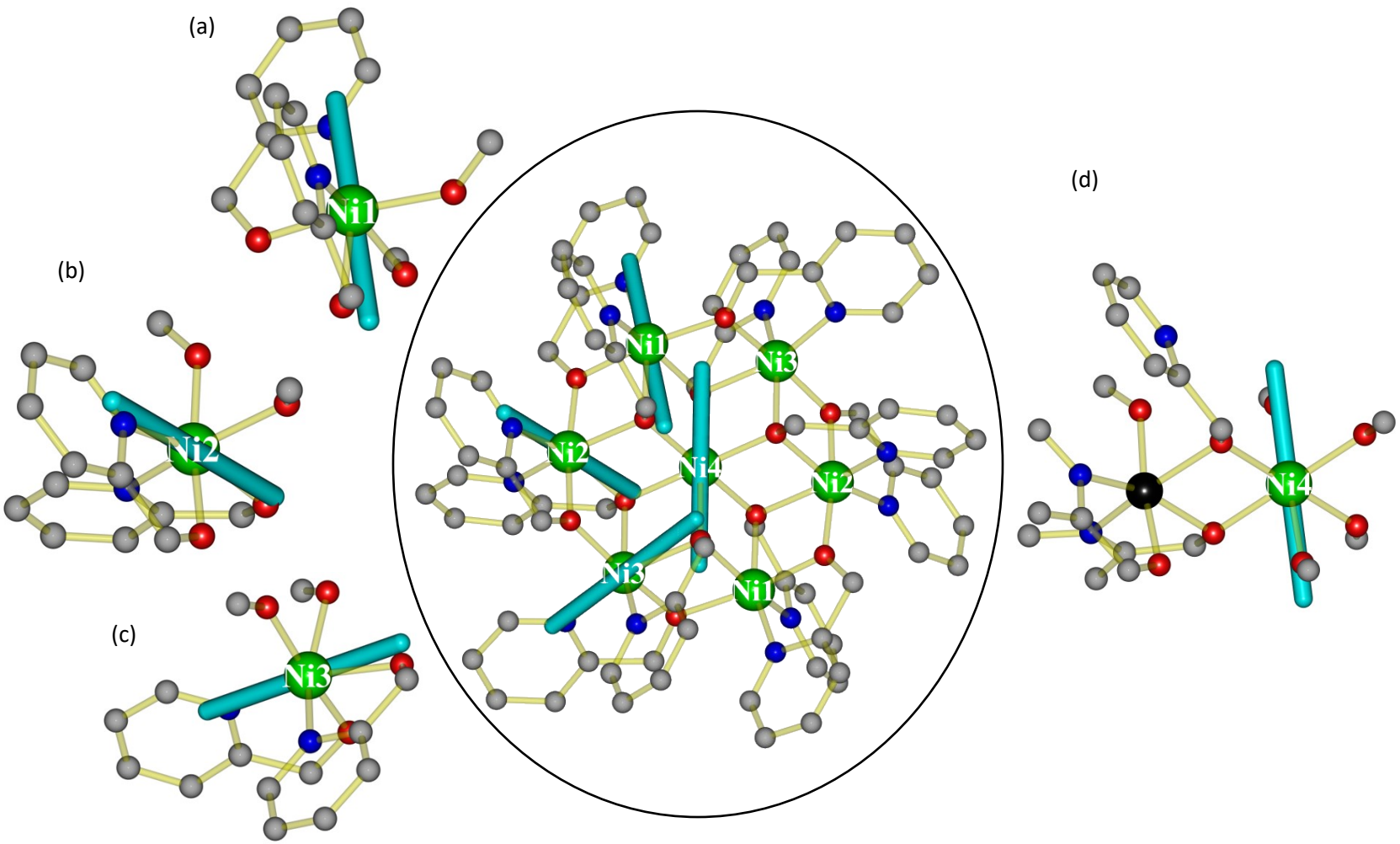

Figure S9. Chemical models used to perform *ab initio* CASSCF/NEVPT2 calculations on the ring Ni(II) and central Ni(II) ions along with the *ab initio* computed D_{zz} axis for the Ni1-Ni4 ions (solid cyan lines). Calculations were performed on the model complexes for Ni1-Ni4 shown on the outside of the central figure (a-d).

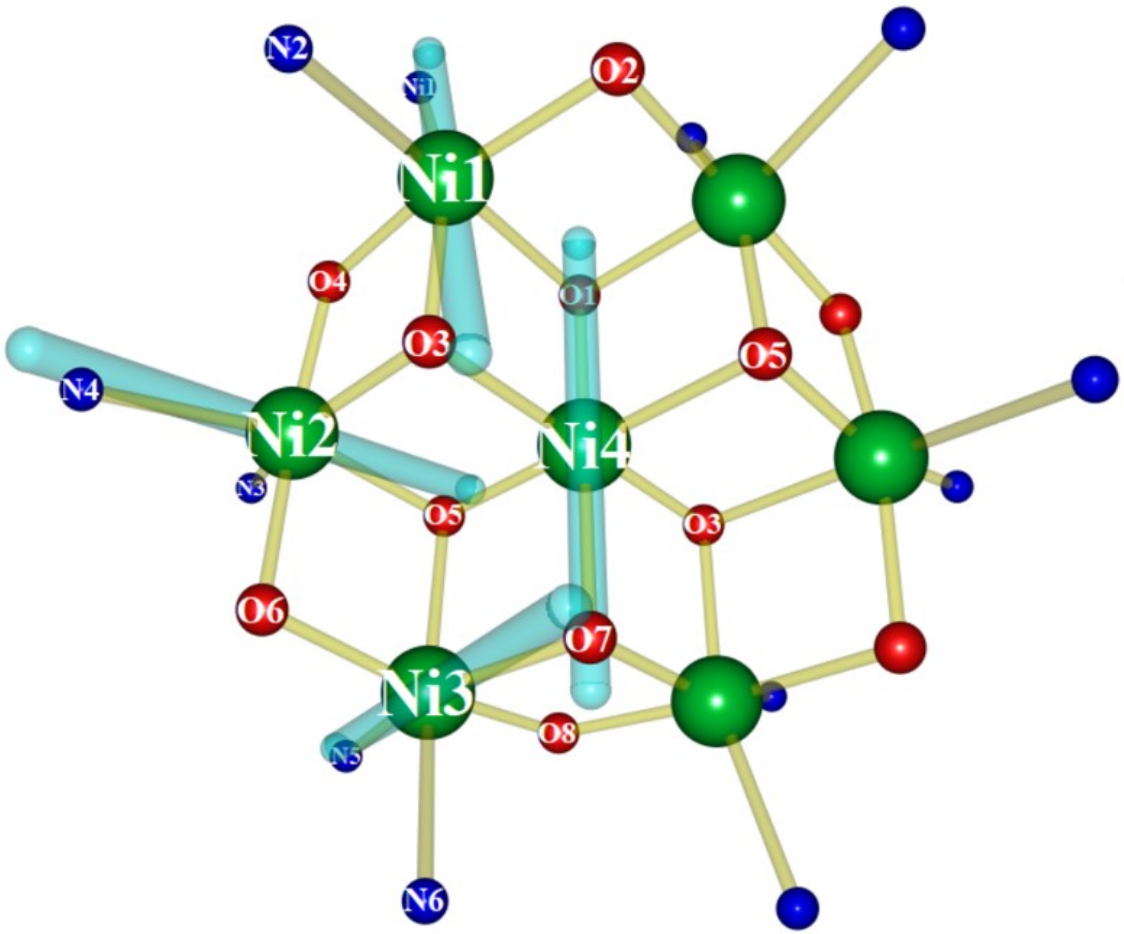

Ni-O/N Distance (Å)	
Ni1-μ_3(O1)	2.125
Ni1-μ_2(O2)	2.019
Ni1-μ_3(O3)	2.056
Ni1-μ_2(O4)	1.989
Ni1-N1	2.025
Ni1-N2	2.049
Ni2-μ_3(O3)	2.119
Ni2-μ_2(O4)	2.001
Ni2-μ_3(O5)	2.048
Ni2-μ_2(O6)	1.984
Ni2-N3	2.042
Ni2-N4	2.020
Ni3-μ_3(O5)	2.107
Ni3-μ_2(O6)	1.999
Ni3-μ_3(O7)	2.055
Ni3-μ_2(O8)	1.999
Ni3-N5	2.028
Ni3-N6	2.053
Ni4-μ_3(O1)	2.086
Ni4-μ_3(O3)	2.073
Ni4-μ_3(O5)	2.072
Ni4-μ_3(O7)	2.086

Figure S10. Chemical core model for complex **1** with the *ab initio* computed D_{zz} axis for the Ni1-Ni4 ions (solid cyan lines) together with Ni(1-4) – N/O distances. Note: the highlighted bonds in the table correspond to the bonds along the D_{zz} axis for the Ni1-Ni4 centres. Note that the direction of D_{zz} axis for Ni1-3 are along the shortest Ni-μ_3O distance, whereas for Ni4, the D_{zz} axis is along the longest Ni-μ_3O distance. The negative and positive sign of the *D* is associated with the compressed and elongated character of the octahedron, respectively.

Table S3. *Ab initio* NEVPT2 calculated anisotropy parameters for the Ni(II) ions of complex **1**, along with the dominant electronic excitations for the first three excitations.

Ni1/Ni5 (D = -7.7 cm^{-1}; E/D = 0.12; g = 2.185, 2.203, 2.250)		
	Contribution to D (cm^{-1})	Dominant transitions
Excitation I	-45.9	$d_{xy} \rightarrow d_{x^2-y^2}$
Excitation II	18.6	$d_{xz} \rightarrow d_{x^2-y^2}$
Excitation III	17.5	$d_{xy} \rightarrow d_{z^2}$
Ni2/Ni6 (D = -7.3 cm^{-1}; E/D = 0.10; g = 2.185, 2.201, 2.245)		
Excitation I	-44.7	$d_{xy} \rightarrow d_{x^2-y^2}$
Excitation II	18.1	$d_{xz} \rightarrow d_{x^2-y^2}$
Excitation III	17.3	$d_{xy} \rightarrow d_{z^2}$
Ni3/Ni7 (D = -5.4 cm^{-1}; E/D = 0.08; g = 2.188, 2.199, 2.236)		
Excitation I	-42.5	$d_{xy} \rightarrow d_{x^2-y^2}$
Excitation II	17.6	$d_{xz} \rightarrow d_{x^2-y^2}$
Excitation III	17.5	$d_{xy} \rightarrow d_{z^2}$
Ni4 (D = 7.3 cm^{-1}; E/D = 0.07; g = 2.227, 2.244, 2.310)		
Excitation I	56.9	$d_{xz} \rightarrow d_{x^2-y^2}/d_{z^2}$
Excitation II-III	- 42.9	$d_{xy} \rightarrow d_{x^2-y^2}/d_{z^2}$

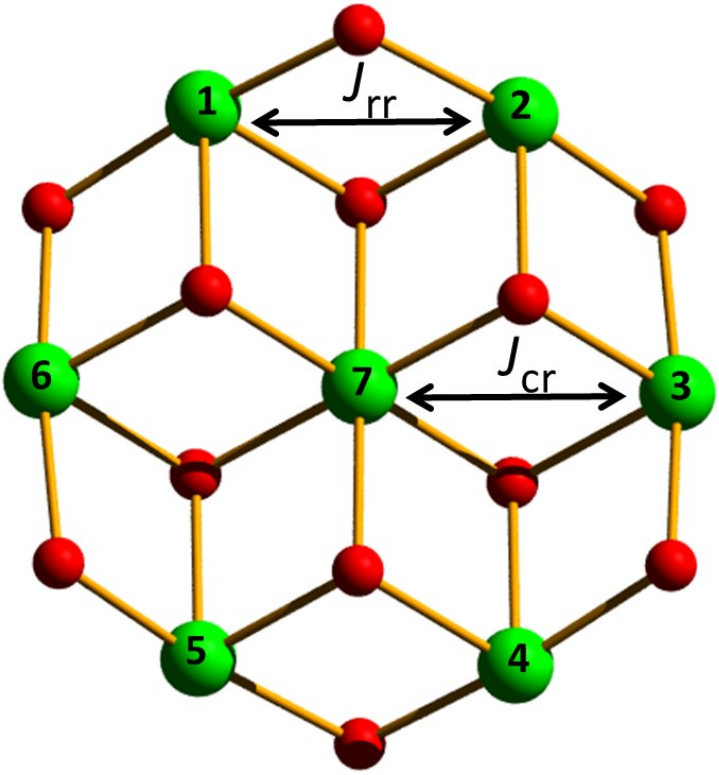

Figure S11. A schematic of the core of **1** with labelling used in the text to construct the magnetic Hamiltonian. In our analysis we have taken a single J_{rr} and a single J_{CR} connecting Ni1-6 to the central Ni7.

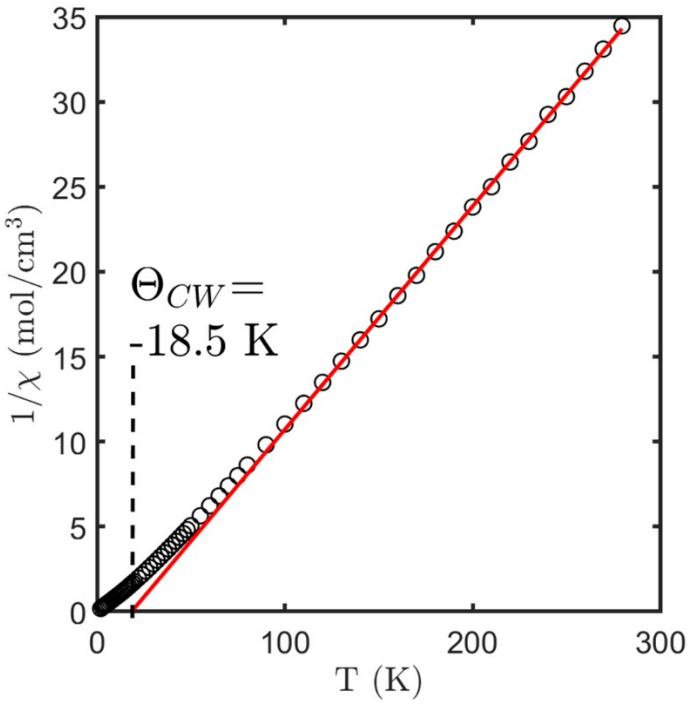

Figure S12. Inverse susceptibility of **1** versus temperature. A fit to a Cure-Weiss function above 90 K is illustrated along with the Cure-Weiss constant, Θ_{CW} = -18.5 K.

References

1. M. J. Frisch, G. W. Trucks, H. B. Schlegel, G. E. Scuseria, M. A. Robb, J. R. Cheeseman, G. Scalmani, V. Barone, G. A. Petersson, H. Nakatsuji, X. Li, M. Caricato, A. V. Marenich, J. Bloino, B. G. Janesko, R. Gomperts, B. Mennucci, H. P. Hratchian, J. V. Ortiz, A. F. Izmaylov, J. L. Sonnenberg, Williams, F. Ding, F. Lipparini, F. Egidi, J. Goings, B. Peng, A. Petrone, T. Henderson, D. Ranasinghe, V. G. Zakrzewski, J. Gao, N. Rega, G. Zheng, W. Liang, M. Hada, M. Ehara, K. Toyota, R. Fukuda, J. Hasegawa, M. Ishida, T. Nakajima, Y. Honda, O. Kitao, H. Nakai, T. Vreven, K. Throssell, J. A. Montgomery Jr., J. E. Peralta, F. Ogliaro, M. J. Bearpark, J. J. Heyd, E. N. Brothers, K. N. Kudin, V. N. Staroverov, T. A. Keith, R. Kobayashi, J. Normand, K. Raghavachari, A. P. Rendell, J. C. Burant, S. S. Iyengar, J. Tomasi, M. Cossi, J. M. Millam, M. Klene, C. Adamo, R. Cammi, J. W. Ochterski, R. L. Martin, K. Morokuma, O. Farkas, J. B. Foresman and D. J. Fox, *Gaussian, Inc., Wallingford CT*, 2016.
2. a) C. Lee, W. Yang and R. G. Parr, *Phys. Rev. B: Condens. Matter*, 1988, **37**, 785; b) A. D. Becke, *J. Chem. Phys.*, 1993, **98**, 5648; c) A. D. Becke, *J. Chem. Phys.*, 1993, **98**, 1372-1377; d) P. J. Stephens, F. J. Devlin, C. F. Chabalowski and M. J. Frisch, *J. Phys. Chem.*, 1994, **98**, 11623-11627.
3. a) A. Schäfer, H. Horn and R. Ahlrichs, *J. Chem. Phys.*, 1992, **97**, 2571; b) A. Schäfer, C. Huber and R. Ahlrichs, *J. Chem. Phys.*, 1994, **100**, 5829; c) G. E. Scuseria and H. F. Schaefer, *III J. Chem. Phys.*, 1989, **90**, 3700.
4. P. C. Hariharan and J. A. Pople, *Theoret. Chim. Acta*, 1973, **28**, 213-222.
5. a) L. Noodleman and D. A. Case, *Adv. Inorg. Chem.*, 1992, **38**, 423; b) L. Noodleman and E. R. Davidson, *Chem. Phys.*, 1986, **109**, 131; c) L. Noodleman, *J. Chem. Phys.*, 1981, **74**, 5737; d) L. Noodleman and J. G. Norman, *J. Chem. Phys.*, 1979, **70**, 4903.
6. F. Neese, *Wiley Interdiscip. Rev. Comput. Mol. Sci.* 2012, **2**, 73–78.
7. (a) K. Eichkorn, O. Treutler, H. Öhm, M. Häser and R. Ahlrichs, *Chem. Phys. Lett.* 1995, **242**, 652–660; (b) K. Eichkorn, F. Weigend, O. Treutler and R. Ahlrichs, *Theor Chem Acc* 1997, **97**, 119–124.
8. (a) C. Angeli, R. Cimiraglia, S. Evangelisti, T. Leininger and J.-P. Malrieu, *J. Chem. Phys.* 2001, **114**, 10252; (b) C. Angeli, R. Cimiraglia and J.-P. Malrieu, *J. Chem. Phys.* 2002, **117**, 9138; (c) C. Angeli, R. Cimiraglia and J.-P. Malrieu, *Chem. Phys. Lett.* 2001, **350**, 297–305.
9. (a) M. K. Singh and G. Rajaraman, *Inorg. Chem.*, 2019, **58**, 3175-3188; (b) M. A. Halcrow, J.-S. Sun, J. C. Huffman and G. Christou, *Inorg. Chem.*, 1995, **34**, 4167-4177; (c) K. K. Nanda, L. K. Thompson, J. N. Bridson and K. Nag, *J. Chem. Soc., Chem. Commun.*, 1994, 1337-1338; (d) L. Ballester, E. Coronado, A. Gutierrez, A. Monge, M. F. Perpinan, E. Pinilla and T. Rico, *Inorg. Chem.*, 1992, **31**, 2053-2056; (e) E. Agapaki, M. K. Singh, A. B. Canaj, G. S. Nichol, J. Schnack and E. K. Brechin, *Chem. Commun.*, 2022, **58**, 9088-9091.
10. (a) A. Sarkar, S. Dey and G. Rajaraman, *Chem. - Eur. J.*, 2020, **26**, 14036-14058; (b) S. K. Singh, T. Gupta, P. Badkur and G. Rajaraman, *Chem. - Eur. J.*, 2014, **20**, 10305.